# Settlement at transition zones in railway tracks is modelling the soil as a 2-D continuum important?

Fărăgău, Andrei B.; Metrikine, Andrei V.; van Dalen, Karel N.

**DOI**
10.1088/1742-6596/2647/8/082019

**Publication date**
2024

**Document Version**
Final published version

**Published in**
Journal of Physics: Conference Series

**Citation (APA)**
Fărăgău, A. B., Metrikine, A. V., & van Dalen, K. N. (2024). Settlement at transition zones in railway tracks: is modelling the soil as a 2-D continuum important? *Journal of Physics: Conference Series*, *2647*(8), Article 082019. https://doi.org/10.1088/1742-6596/2647/8/082019

**Important note**
To cite this publication, please use the final published version (if applicable).
Please check the document version above.

Journal of Physics: Conference Series **2647** (2024) 082019 doi:10.1088/1742-6596/2647/8/082019

# Settlement at transition zones in railway tracks – is modelling the soil as a 2-D continuum important?

**Andrei B. Fărăgău, Andrei V. Metrikine, Karel N. van Dalen**

Faculty of Civil Engineering and Geosciences, Delft University of Technology, the Netherlands

E-mail: a.b.faragau@tudelft.nl

**Abstract.** While most recent models of railway tracks include the nonlocal nature of the foundation reaction force, few studies have investigated the influence of its nonlocal nature on the response. Accounting for the nonlocal nature of the foundation force is computationally expensive and increases the complexity of the model, thus, knowing when and when not to account for it is important. This paper aims to shed light on the influence of the nonlocal, both in time and space, reaction force provided by the foundation on the transient response at railway transition zones. To this end, a 2-D system in which the soil layer is modelled as a visco-elastic continuum is compared to an equivalent 1-D system with a local foundation reaction force (i.e., Winkler foundation). Results show that, in general, the response of the 2-D system with shallow and/or stiff soil layers can be well captured by the equivalent 1-D model. However, for medium-to-deep and/or soft soil layers, the nonlocality of the foundation reaction force is influential and the transient response at transition zones cannot be satisfactorily captured by 1-D models. Finally, the ballast settlement is also poorly captured for medium-to-deep and/or soft soil layers, with the main cause being the inability of the 1-D model to separate between ballast and soil stresses, and not the locality of the reaction force.

## 1. Introduction

With the increasing demand on railway transport due to its capability of operating fully on sustainable energy, the previously considered acceptable deterioration of the infrastructure is rapidly becoming a limiting factor in its sustainable development. One such situation is encountered at track transition zones found near structures such as bridges and tunnels, which exhibit a significant variation of track properties (e.g., foundation stiffness). These zones require more maintenance than the rest of the track as they are prone to pronounced differential settlements. In general, the measures to counteract these differential settlements were not successful, some due to poor design or deficient implementation, but the majority due to the lack of understanding of the governing mechanisms that cause the pronounced differential settlements.

To identify and investigate the underlying degradation mechanisms, next to experimental investigations, researchers and engineers used computational models ranging from simple phenomenological 1-D/2-D models (e.g., [1, 2, 3, 4]) to complex predictive 2-D/3-D models (e.g., [5, 6, 7, 8, 9]). While the latter are important in situations when specific predictions

are required, the interference and interaction of multiple phenomena makes it difficult to study specific mechanisms in detail, for which the former models are sometimes preferred. Nonetheless, these phenomenological 1-D models have drawbacks, one of which being the local nature of the foundation reaction-force.

The nonlocal nature of the foundation reaction force has been incorporated in numerous models of railway tracks. For example, all models that consider the multi-dimensionality of the problem as well as the 1-D models that consider multiple components in vertical direction (e.g., [10]) have a nonlocal reaction force as experienced at the rail level. However, most of these models do not specifically investigate the influence of reaction force nonlocality. The studies that do investigate this, for example [11, 12, 10], are all concerned with the influence of reaction force nonlocality on the steady-state regime. The current investigation aims to shed light on the influence of the nonlocal, both in time and space, reaction force provided by the foundation for the transient response at transition zones. Furthermore, situations are distinguished in which accounting for it is necessary for accurate predictions of settlement at transition zones. This study can help researchers and engineers in better understanding the limitations of simplified modelling approaches depending on the specific problem investigated.

To study the influence of the nonlocal foundation reaction force on the transient response at transition zones, the response of the a 2-D system is compared to an equivalent 1-D system with a local foundation reaction force. The two models are schematically presented in Fig. 1. The railway track is modelled as a beam on a nonlinear and inhomogeneous spring-dashpot layer (i.e., Kelvin layer) in the 1-D system, similar to the models formulated in [3, 13], while the 2-D system incorporates additionally a soil layer of depth $Z$ modelled as an elastic continuum; both models are subject to a moving constant load. The track periodicity induced by the sleepers is neglected because the response amplification caused by the mechanisms observed in Ref. [14] is minimal for the railway track. The settlement and variation of track properties is restricted to the Kelvin layer, as the soil-layer continuum is assumed to be linear and homogeneous. The simplistic geometry of the 2-D system formulated here is ideal for investigating the influence of the nonlocality since the only difference between the two models is the addition of the soil layer. Note that the results are not compared to site measurements to determine if the continuum is a good representation of the soil; we assume a-priori that the 2-D system with a nonlocal foundation force is a more accurate description of reality.

The nonlinear constitutive model of the Kelvin foundation is representative of settlement occurring in the ballast layer, and is described in Ref. [3]. It is important to note that this constitutive model only captures the additional settlement due to response amplification at transition zones and does not account for the settlement that occurs in quasi-homogeneous sections of the track. This scope limitation implies that we focus on large load velocities at which the response amplification at transition zones is significant. To determine the solution of the inhomogeneous and nonlinear systems described above, the so-called pseudo-force method is used, which is thoroughly described in Ref. [13] and is not repeated here for brevity.

## 2. Influence of reaction-force nonlocality

The equation of motion of the linear and homogeneous 1-D model in the absence of an external load in both the time-space ($t$ and $x$) and frequency-wavenumber ($\omega$ and $k_x$) domains, reads

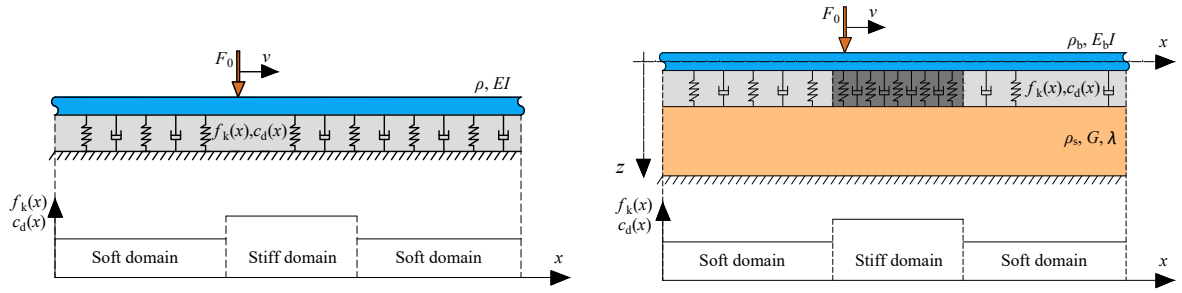


Figure 1: Schematic representation of the 1-D (left panel) and 2-D (right panel) models.

(damping is neglected for simplicity)

$$EIw'''' + \rho\ddot{w} + k_\mathrm{d}w = 0, \tag{1}$$

$$\overline{\chi}_{1\mathrm{D}}\overline{w} = 0, \qquad \overline{\chi}_{1\mathrm{D}} = EIk_x^4 - \rho\omega^2 + k_\mathrm{d}, \tag{2}$$

where $k_\mathrm{d}$ is the distributed spring stiffness, $EI$ the bending stiffness, $\rho$ the mass of the beam, $w$ the displacement of the beam, $\overline{\chi}_{1\mathrm{D}}$ is the equivalent dynamic stiffness of the complete 1-D system, the overline represents the quantity in the frequency-wavenumber domain, and primes and overdots represent partial derivatives in space and time, respectively. The corresponding equations for the 2-D model read

$$EIw'''' + \rho\ddot{w} + \int_{-\infty}^{\infty}\int_{-\infty}^{t} \chi_{\mathrm{f,2D}}(x-\xi, t-\tau)w(\xi,\tau)\mathrm{d}\tau\mathrm{d}\xi = 0, \tag{3}$$

$$\overline{\chi}_{2\mathrm{D}}\overline{w} = 0, \qquad \overline{\chi}_{2\mathrm{D}} = EIk_x^4 - \rho\omega^2 + \overline{\chi}_{\mathrm{f,2D}}, \qquad \overline{\chi}_{\mathrm{f,2D}} = \frac{k_\mathrm{d}\overline{\chi}_\mathrm{s}(k_x,\omega)}{k_\mathrm{d} + \overline{\chi}_\mathrm{s}(k_x,\omega)}, \tag{4}$$

where (i) $\overline{\chi}_{2\mathrm{D}}$, (ii) $\overline{\chi}_{\mathrm{f,2D}}$, and (iii) $\overline{\chi}_\mathrm{s}$ are the equivalent dynamic stiffnesses of the (i) complete 2-D system as experienced at the beam level, (ii) foundation (spring and soil layers combined; $\chi_{\mathrm{f,2D}}$ is its time-space domain counterpart), and (iii) soil layer at the top surface. The expression of $\overline{\chi}_\mathrm{s}$ is not presented here for brevity, but can be obtained analytically as done in Ref. [11].

Comparing the foundation stiffnesses, $k_\mathrm{d}$ in the 1-D model and $\overline{\chi}_{\mathrm{f,2D}}(\omega, k_x)$ in the 2-D model, highlights the difference between the two models. The locality of the Winkler foundation results in its stiffness to be independent of the frequency and wavenumber of waves travelling in the system. The 2-D model, on the other hand, includes both history effects through time nonlocality, as well as spatial nonlocality, both introduced through convolution integrals. In other words, the foundation reaction force in the 2-D system is both frequency and wavenumber dependent. It is important to emphasize that by considering an elastic continuum, the reaction force becomes nonlocal in both time (history effects) and space. Other works introduce the spatial (e.g., [15, 16]) and temporal (e.g., [17]) nonlocality independently. While the spatial or the temporal nonlocality can be more or less influential depending on the specific application, separating the two is not desired since frequency and wavenumber are fundamentally interlinked in waves, and separating them would be, in principle, physically incorrect.

Fig. 2 presents the equivalent stiffnesses (i.e., soil layer, soil-Winkler combination, and soil-Winkler-beam combination) of the 2-D system with different soil depths for long (left panel)

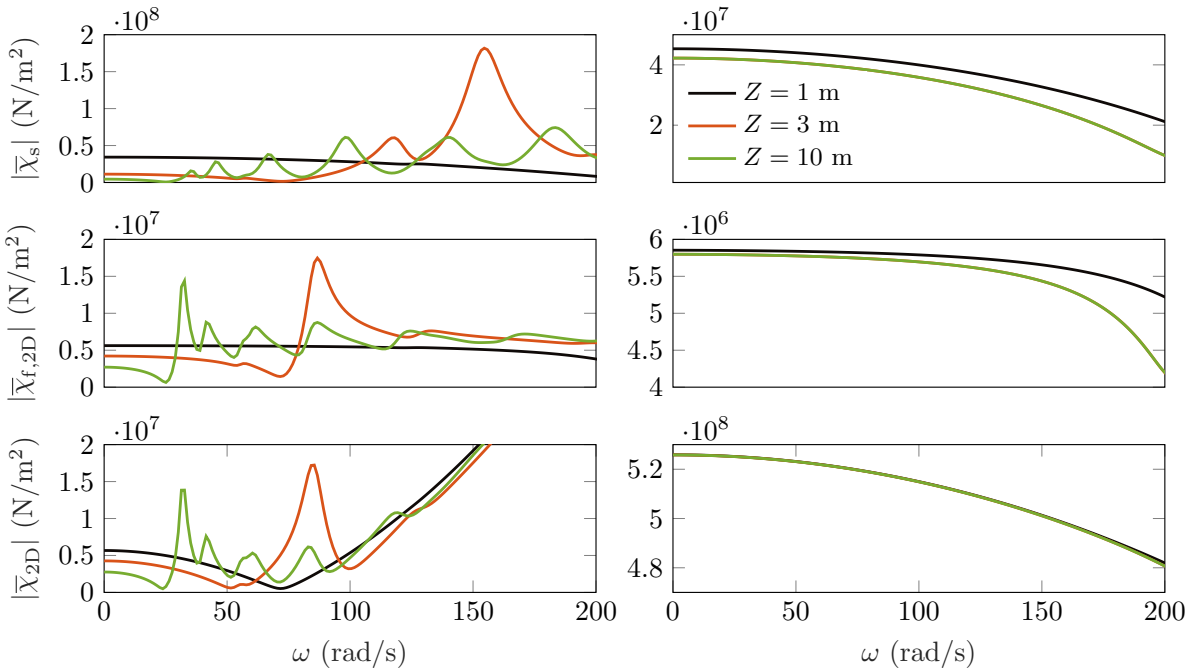


Figure 2: The equivalent stiffnesses of (i) the 2-D soil layer at the surface (top panels), (ii) the combined soil layer and the Winkler foundation (middle panels), and (iii) the complete 2-D system including the beam (bottom panels) for different layer depths and for long waves (left panels) and short waves (right panels).

and short (right panel) waves travelling along the waveguide. For short waves (right panels), the variation of the equivalent stiffnesses with frequency and soil-layer depth is small and monotonic. The wave is sufficiently short to completely vanish at the bottom of the layer even for $Z = 1$ m; consequently, increasing the layer depth does not have a considerable influence. For long waves (left panels), the following observations can be made:

(i) When it comes to the soil layer only, for an extremely shallow soil layer (e.g., $Z = 1$ m), $\overline{\chi}_s$ does not vary considerably in the frequency range of interest (for ground vibrations). However, as the soil-layer depth increases, $\overline{\chi}_s$ varies greatly as an increasing number of soil-layer modes are located in this frequency range. However, even though more modes are visible, increasing the soil-layer depth leads to a reduced amplification of $\overline{\chi}_s$ at these modes (i.e., the green peaks in the top left panel of Fig. 2 are smaller than the orange ones).

(ii) Adding the Winkler layer leads to a reduction i both amplitude and variation of the equivalent stiffness $\overline{\chi}_{f,2D}$ compared to $\overline{\chi}_s$, especially at relatively high frequencies ($\omega = 100$–$200$ rad/s). This is favourable for the 1-D model, since the smaller the stiffness variation, the more accurately it can be approximated by a local foundation. The ratio of the spring stiffness to the soil stiffness is important though; for a very stiff Winkler layer, $\overline{\chi}_{f,2D}$ is very similar to $\overline{\chi}_s$, both in magnitude and shape, while for a very soft Winkler layer, $\overline{\chi}_{f,2D}$ is very similar to $k_d$ as the soil layer acts as a rigid bottom due to it being much stiffer than the Winkler layer.

(iii) The addition of the beam has a small effect at low frequencies and wavenumbers, but dominates the equivalent stiffness at relatively large frequencies and wavenumbers, at which

the soil-layer depth seems to be insignificant for $\overline{\chi}_{2D}$. This shows that, with the addition of the beam, the influence of foundation force nonlocality is negligible above a certain frequency.

Qualitatively similar observations can be made for varying the soil stiffness. Increasing the soil-layer depth is, to some extent, qualitatively equivalent to reducing the soil stiffness, and vice-versa. These results are not presented here for brevity.

From this analysis, the difficulty of capturing the soil reaction force through a local (i.e., frequency and wavenumber independent) force for a wide range of frequencies, wavenumbers, material properties, and system geometry (e.g., soil depth) becomes clear. However, with the addition of the Winkler layer and the beam, the nonlocality of the reaction force on the equivalent stiffness as experienced by the vehicle is reduced significantly. Therefore, the tuning of the 1-D model should focus on capturing the equivalent stiffness as experienced by the vehicle. This is done in the next section.

## 3. Steady state response

For a meaningful comparison, the 1-D model must be tuned to the 2-D one. The 1-D model essentially has three parameters to tune, namely the mass of the beam and the stiffness and damping of the Kelvin layer. The bending stiffness was initially included as a tuning parameter, but we observed that it did not change significantly. Therefore, we choose to assign it the same value as in the 2-D model.

Tuning of simplified (1-D) railway track models to more sophisticated models or field measurements is usually performed using the steady-state response in the time domain (e.g., [10, 8]). Tuning the steady state comes down to tuning the equivalent stiffness $\overline{\chi}_{2D}$ along the kinematic invariant $\omega = k_x v$. This procedure is usually done for one load velocity and results computed for the similar velocities, generally leading to good agreements. We choose a different tuning procedure, namely to allow more discrepancy in the steady-state fields for each specific velocity, but to obtain a better match over the whole dynamic velocity regime ($v \approx 0.5$–$1$ $c_{\mathrm{cr}}$, where $c_{\mathrm{cr}}$ is the lowest critical velocity in the 2-D system). This way, more of the physically relevant properties of the system, such as the cut-off frequency and critical velocity, are captured reasonably well. Moreover, since this paper focuses on the settlement that mostly develops under the moving load [3, 8], the steady-state displacement under the moving load is used as the objective function. A least-squares optimization algorithm is used for the tuning procedure. The values obtained for a soil depth $Z = 3$ m are given in Appendix A and the comparison is presented in Fig. 3.

Fig. 3 compares the steady-state displacement under the moving load in both models and presents the associated relative error for the dynamic velocity regime. The responses under the moving load show a good agreement with an overall relative error $e = \frac{|w_{2D} - w_{1D}|}{|w_{2D}|}$ below 3–4% for all soil depths considered, and the critical velocities are also well captured. The poor match at super-critical velocities is not of concern since we focus on sub-critical velocities. The bottom panels compare the steady-state displacement fields of the two models for a velocity $v \approx 0.75 c_{\mathrm{cr}}$. It can be seen that the steady-state displacement fields match very well for $Z = 1$ m, while they show a poor agreement for $Z = 10$ m, even though the response under the moving load has a small relative error. This was to be expected from the observations made in the previous section; the local reaction force is tuned such that the responses under the moving load match,

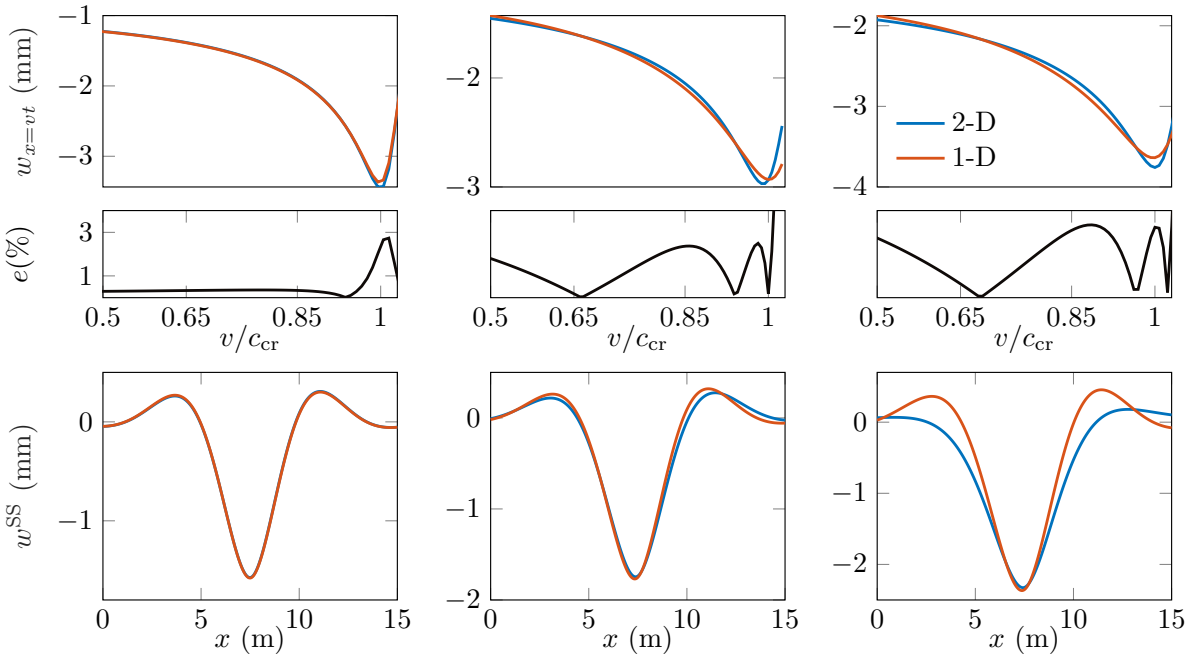


Figure 3: Comparison of the steady-state displacement under the moving load versus load velocity (top panels), the relative error (middle panels), and the steady-state displacement fields for $v \approx 0.75c_{\mathrm{cr}}$ (bottom panels) for $Z = 1$ m (left panels), $Z = 3$ m (centre panels), and $Z = 10$ m (right panels). The results are for the soft domain, and qualitatively similar results are obtained for the stiff domain.

but it fails to capture the correct response for all other frequencies and wavenumbers. It can also be seen that the foundation nonlocality tends to spread the displacement profile over a larger distance compared to the local foundation, leading to a broader and less wavy profile.

It is important to mention that tuning the steady-state displacement fields for one specific velocity leads to a much better agreement of the response fields, but the relevant physical properties of the system are lost and the agreement for slightly different velocities than the tuning one is much worse. In principle, a good agreement of the steady-state responses for one velocity does not necessarily translate to a good agreement of the transient response too. This is investigated in the next sections, where the two systems are compared in terms of transient response fields as well as through dispersion curves and predicted settlement.

## 4. Transient response

Fig. 4 compares the steady-state and free-field responses of the 1-D and 2-D models in the frequency domain for different soil-layer depths. The responses are evaluated 1 m to the left of the stiff zone where the interference of the two fields (steady state and free field) is most pronounced. As expected from the previous section, for the extremely shallow soil layer (i.e., $Z = 1$ m) both the steady-state and free-fields show a good agreement because the nonlocal reaction force has an insignificant variation in the frequency range of interest (see Fig. 2). While in the case of $Z = 3$ m, the agreement is acceptable, for $Z = 10$ m there is barely any agreement,

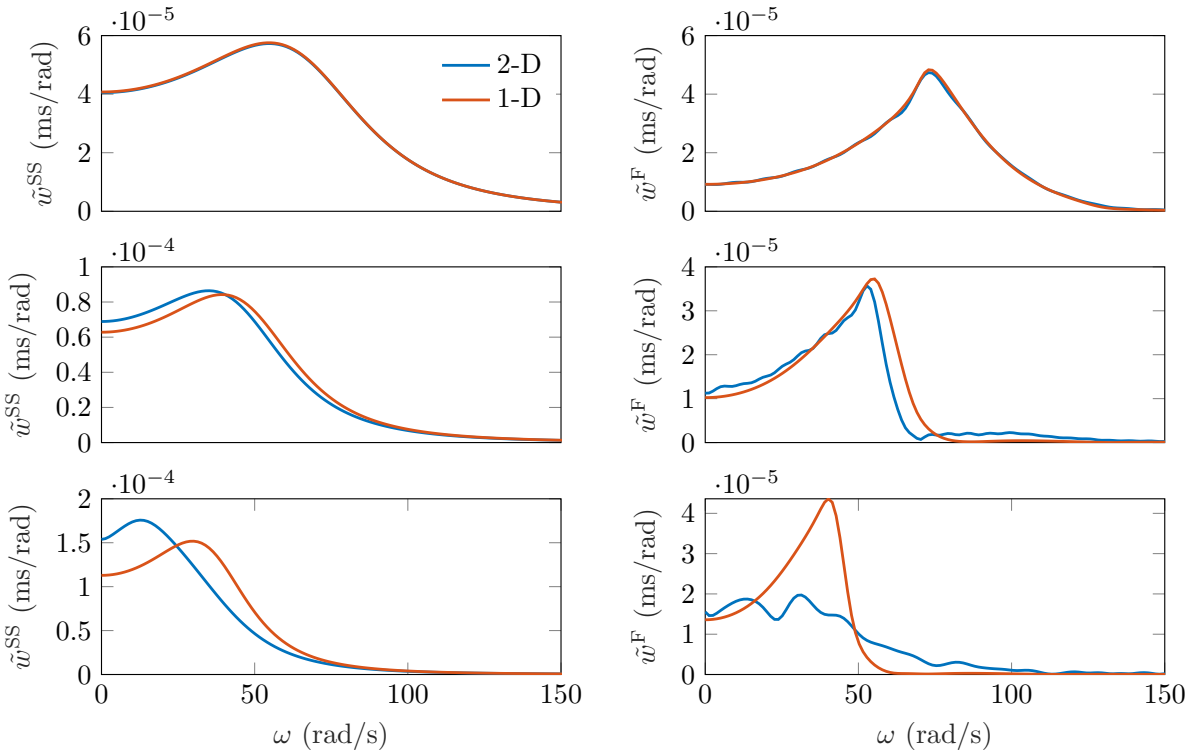


Figure 4: The frequency spectra of the eigenfields $\tilde{w}^{\mathrm{SS}}$ (left panels) and of the free-fields $\tilde{w}^{\mathrm{F}}$ (right panels) for $Z = 1$ m (top panels), $Z = 3$ m (middle panels), and $Z = 10$ m (bottom panels). The responses are evaluated 1 m to the left of the stiff zone.

especially for the free field. Qualitatively, the same results are observed at the right-side of the transition zone, and those results are not presented here for brevity.

As can be seen in Fig. 4, the main content of the free-field spectrum is at same frequency range as the eigenfield. Consequently, one might assume that tuning the 1-D model to the 2-D one based on the eigenfields, the free field (and thus the total transient field) is also well captured. However, this is not always the case. The fact that the equivalent stiffness of the 2-D soil layer is frequency-wavenumber dependent leads to the 2-D system to allow infinitely more waves to exist. This is best exemplified through the dispersion curves presented in Fig. 5 for $Z = 3$ m. It can be seen that while the 1-D system allows for two waves (two dispersion curves), the 2-D system has significantly more dispersion branches (actually it has infinitely many, but only a finite amount are presented). The tuning of the 1-D system has led to a good agreement of the dispersion curves in a limited frequency-wavenumber region (indicated by the green rectangles)[1]. However, the good match is only for two of the dispersion branches (one real-valued and one complex-valued); since the classical 1-D model does not have more than two dispersion curves, it fails to capture the multitude of evanescent waves that the 2-D model allows for, and it completely misses the purely-imaginary branches indicated through the red rectangle that are influential in the vicinity of the transition zone.

[1] The range in which the dispersion curves match can be adjusted; for example, if the tuning was done for the quasi-static velocity regime, the good match would be at slightly lower frequencies.

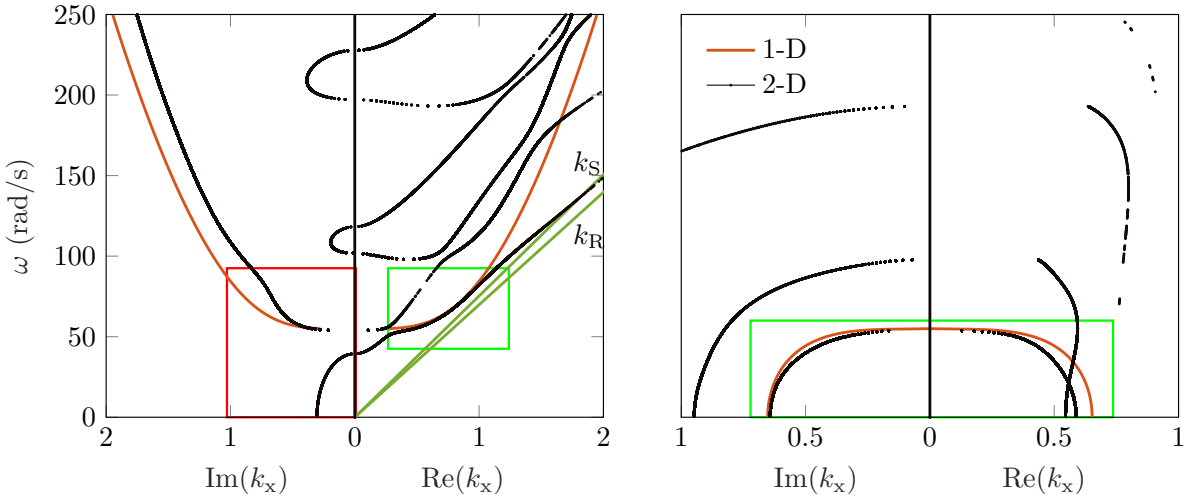


Figure 5: Dispersion curves of the undamped 2-D and 1-D systems. The left panel present the purely real- and imaginary-valued wavenumbers while the right panels present the complex-valued wavenumbers. $k_S$ and $k_R$ are the shear and Rayleigh wavenumbers, respectively; $Z = 3$ m.

## 5. Settlement after one load passage

The observed difference in the free field (Fig. 4), especially for large soil-layer depths, strongly affects the settlement predicted by the two models. The current work considers only the settlement caused by the response amplification at transition zones and neglects the ballast settlement far away from these zones. Consequently, correctly capturing not only the eigenfield, but also the free field is paramount in accurately predicting settlement.

Figure 6 presents the settlement profile obtained with both models, for different soil depths, after one load passage. Results show that the degradation in the 1-D model is significantly larger than in the 2-D model for all soil-layer depths considered. The discrepancies in the settlement magnitude are caused by two factors: partly due to (i) the nonlocality of the reaction force, but mostly due to (ii) the fact that the 2-D model separates the ballast and soil layers, and therefore can capture the stresses in the ballast, while the 1-D model does not separate the two. As a consequence of (ii), the settlement in the 1-D model is based on the displacement of the beam, while in the 2-D model it is dictated by the differential displacement between the beam and the top surface of the soil. Since the soil is considerably softer than the ballast, the differential settlement between the beam and the top surface of soil is small, leading to a reduced settlement. This shows that if the settlement magnitude is to be correctly predicted, it is more important to account for the flexible bottom of the Kelvin layer than to introduce the foundation nonlocality.

## 6. Conclusions

This paper studied the influence of the nonlocal foundation reaction force on the transient response at railway track transition zones. This was done by comparing a 2-D system, in which the soil layer is modelled as a visco-elastic continuum, to an equivalent 1-D system with a local foundation reaction force (i.e., Winkler foundation).

It was shown that the nonlocality of the foundation reaction force is influential for systems with soft/deep soil layers, and can be neglected for shallow/stiff layers. For a medium-to-deep

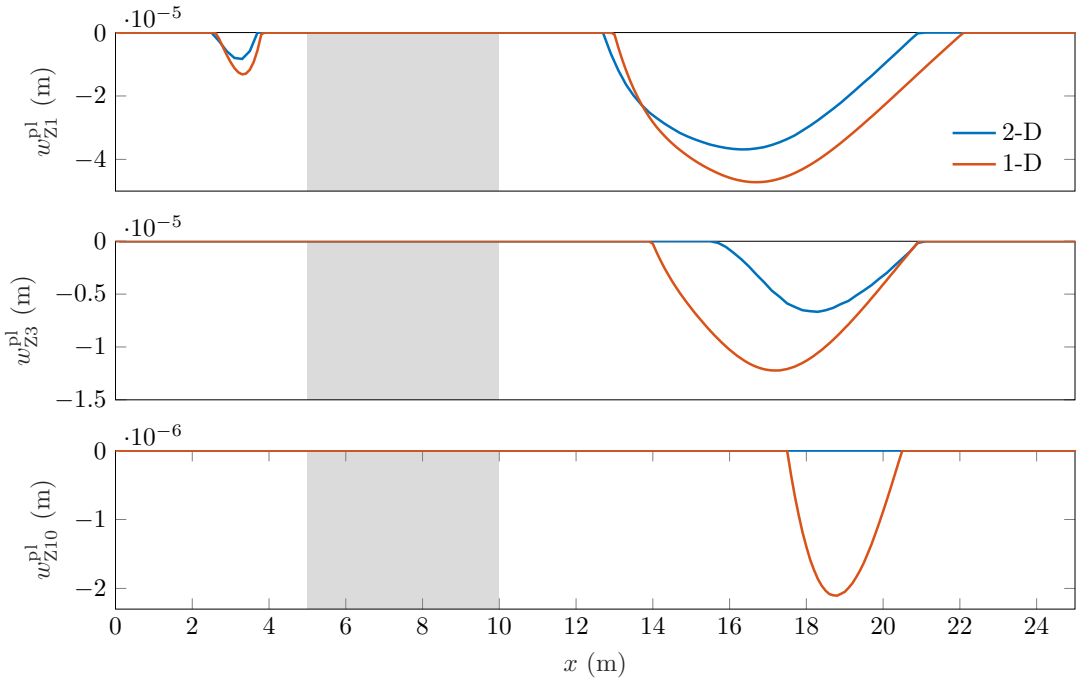


Figure 6: The settlement predicted by the two models after one passage of the load for $Z = 1$ m (top panel), $Z = 3$ m (middle panel), and $Z = 10$ m (bottom panel). The stiff zone is represented through the grey background.

soft layer, the 1-D local model fails to capture the many different evanescent modes that are present in the 2-D system, leading to the transient behaviour to be poorly captured by the 1-D model. The settlement predicted by the 1-D local model is also poorly captured for a medium-to-deep soft layer, partly due to the local reaction force, but mostly due to the 1-D model not being able to separate between the stresses in the ballast and in the soil. These represent two important limitations of this 1-D model and shows that it is difficult, if not impossible, to accurately predict both the eigenfield and of the free field as well as the settlement at transition zones.

## References

[1] Varandas J N, Hölscher P and Silva M A G 2014 *Proceedings of the Institution of Mechanical Engineers, Part F: Journal of Rail and Rapid Transit* **228** 242–259 ISSN 09544097
[2] Nielsen J C and Li X 2018 *Journal of Sound and Vibration* **412** 441–456 ISSN 10958568 URL `https://doi.org/10.1016/j.jsv.2017.10.005`
[3] Fărăgău A B, Metrikine A V and van Dalen K N 2019 *Nonlinear Dynamics* **98** 2435–2461
[4] Nasrollahi K, Nielsen J C, Aggestam E, Dijkstra J and Ekh M 2022 *Lecture Notes in Mechanical Engineering* **283** 282–292 ISSN 21954364 URL `https://doi.org/10.1016/j.engstruct.2023.115830`
[5] Wang H and Markine V 2019 *Journal of Sound and Vibration* **459** ISSN 10958568 URL `https://doi.org/10.1016/j.jsv.2019.114863`
[6] Varandas J N, Paixão A, Fortunato E, Zuada Coelho B and Hölscher P 2020 *Computers and Geotechnics* **126** 103712 ISSN 18737633 URL `https://doi.org/10.1016/j.compgeo.2020.103712`
[7] Paixão A, Varandas J N and Fortunato E 2021 *Frontiers in Built Environment* **7** 1–16 ISSN 22973362
[8] de Oliveira Barbosa J M, Fărăgău A B and van Dalen K N 2021 *Journal of Sound and Vibration* **494** ISSN 10958568

[9] de Oliveira Barbosa J M, Fărăgău A B, van Dalen K N and Steenbergen M 2022 *Journal of Sound and Vibration* **530** 116942 ISSN 0022460X
[10] Rodrigues A F S and Dimitrovová Z 2021 *Vibration* **4** 151–174
[11] Dieterman H A and Metrikine A V 1996 *Eur. J. Mech. A/Solids* **15** 67–90
[12] Dieterman H A and Metrikine A V 1997 *European Journal of Mechanics, A/Solids* **16** 295–306 ISSN 09977538
[13] Fărăgău A B, Keijdener C, de Oliveira Barbosa J M, Metrikine A V and van Dalen K N 2021 *Nonlinear Dynamics* **103** 1365–1391
[14] Fărăgău A B, de Oliveira Barbosa J M, Metrikine A V and van Dalen K N 2022 *Mathematics and Mechanics of Solids* 1–21
[15] Versteijlen W G, de Oliveira Barbosa J M, van Dalen K N and Metrikine A V 2018 *International Journal of Solids and Structures* **134** 272–282 ISSN 00207683 URL `https://doi.org/10.1016/j.ijsolstr.2017.11.007`
[16] Tsetas A, Tsouvalas A and Metrikine A V 2021 *Journal of Marine Science and Engineering* **9** ISSN 20771312
[17] Kementzetzidis E, Pisanò F and Metrikine A V 2022 *Computers and Geotechnics* **148** 104810 ISSN 18737633 URL `https://doi.org/10.1016/j.compgeo.2022.104810`

## Appendix A. Parameter values

It must be emphasized that this paper focuses on qualitative analyses for which the exact parameter values are not of crucial importance. Nonetheless, we want to investigate the responses of the two systems in a realistic parameter space. To this end, the parameter values of the 2-D system are selected such that its steady-state response resembles the one of an equivalent 3-D FEM model (the description of this model is not presented here for brevity). The Kelvin layer, theoretically, represents the vertical stiffness and damping of the rail-pads ($k_{\mathrm{d,rp}}$) and ballast ($k_{\mathrm{d,bal}}$). However, we do not make an explicit distinction between them and the Kelvin layer was tuned such that, using the previously defined values for the soil and moving load, the magnitude of the responses in the 3-D and 2-D models are similar (the bending stiffness of the beam is the same as in the 3-D model). As for the damping of the Kelvin layer, a conservative ratio $\zeta_{\mathrm{K}}$ of 5% has been chosen since most amount of damping in this system is expected to come from the soil and not from the ballast layer. Finally, the mass of the ballast $\rho_{\mathrm{bal}}$ (next to the mass of the sleepers $\rho_{\mathrm{slp}}$ and of the rail $\rho_{\mathrm{r}}$) is included in the linear mass of the beam (i.e., $rho_b = \rho_{\mathrm{r}} + \rho_{\mathrm{slp}} + \rho_{\mathrm{bal}}$). The parameter values are given in Table A1

The parameter values of the 1-D model are tuned such that its response under the moving load matches the response of the 2-D model in the dynamic velocity regime (see Section 3 and Fig. 3). The values obtained for the 1-D model are presented in Table A2.

Table A1: Values of the system parameters used in this paper.

| Parameter | Symbol | Value | Unit |
|---|---|---|---|
| Bending stiffness | $EI$ | $6.42{\cdot}10^6$ | $\mathrm{Nm}^2$ |
| Rail mass | $\rho_\mathrm{r}$ | 60 | kg/m |
| Distributed half-sleeper mass | $\rho_\mathrm{slp}$ | 208.33 | kg/m |
| Half-layer of ballast mass | $\rho_\mathrm{bal}$ | 810 | kg/m |
| Moving-load magnitude | $F_0$ | $18 \cdot 10^3$ | N |
| Kelvin layer stiffness | $k_\mathrm{d}$ | $6.7{\cdot}10^6$ | $\mathrm{N/m}^2$ |
| Kelvin damping ratio | $\zeta_\mathrm{K}$ | 0.05 | |
| Soil shear modulus | $G$ | $10 \cdot 10^6$ | $\mathrm{N/m}^2$ |
| Soil mass density | $\rho_\mathrm{s}$ | 1730 | $\mathrm{kg/m}^3$ |
| Poisson ratio | $\nu$ | 0.3 | |
| Soil damping factor | $\zeta_\mathrm{s}$ | 0.1 | |
| Layer depth | $Z$ | 3 | m |
| Elastic displacement limit ratio | $\Delta w_\mathrm{el}/\Delta w^\mathrm{e}_\mathrm{max}$ | 1.02 | |

Table A2: The tuned values of the parameters of the 1-D model for $Z = 3$ m.

| Parameter | Symbol | Value | Unit |
|---|---|---|---|
| Beam mass–soft domain | $\rho_\mathrm{l}$ | 1550 | kg/m |
| Kelvin stiffness–soft domain | $k_\mathrm{d,l}$ | $4.7{\cdot}10^6$ | $\mathrm{N/m}^2$ |
| Kelvin damping–soft domain | $c_\mathrm{d,l}$ | $1.3{\cdot}10^4$ | $\mathrm{Ns/m}^2$ |
| Beam mass–stiff domain | $\rho_\mathrm{r}$ | 2540 | kg/m |
| Kelvin stiffness–stiff domain | $k_\mathrm{d,r}$ | $1.2{\cdot}10^7$ | $\mathrm{N/m}^2$ |
| Kelvin damping–stiff domain | $c_\mathrm{d,r}$ | $2.4{\cdot}10^4$ | $\mathrm{Ns/m}^2$ |